PAPER

Conditional recurrence plots for the investigation of sawteeth pacing with RF modulation

IOP Publishing Plasma Physics and Controlled Fusion
Plasma Phys. Control. Fusion **64** (2022) 084002 (7pp) https://doi.org/10.1088/1361-6587/ac757c

Conditional recurrence plots for the investigation of sawteeth pacing with RF modulation

Emmanuele Peluso[1,*], Andrea Murari[2], Teddy Craciunescu[3], Ernesto Lerche[4,5], Pasquale Gaudio[1], Michela Gelfusa[1], Daniel Gallart[6], David Taylor[7] and JET Contributors[8]

[1] Department of Industrial Engineering, University of Rome 'Tor Vergata', via del Politecnico 1, 00133 Roma, Italy
[2] Consorzio RFX (CNR, ENEA, INFN, Universita' di Padova, Acciaierie Venete SpA), Corso Stati Uniti 4, Padova, Italy
[3] National Institute for Laser, Plasma and Radiation Physics, Magurele-Bucharest, Romania
[4] Euratom/CCFE Fusion Association, Culham Science Centre, Abingdon, United Kingdom
[5] LPP-ERM/KMS, Association EUROFUSION-Belgian State, TEC Partner, Brussels, Belgium
[6] Barcelona Supercomputing Center (BSC), 08034 Barcelona, Spain
[7] Culham Centre for Fusion Energy, Oxford, United Kingdom

E-mail: emmanuele.peluso@uniroma2.it

Received 14 February 2022, revised 10 May 2022
Accepted for publication 1 June 2022
Published 24 June 2022

Abstract

In many areas of research, from neurobiology to nuclear fusion, which investigate complex dynamical systems involving numerous, different and interconnected physical quantities, the application of advanced analysis tools based on Chaos theory and Information theory has provided significant improvements both by supporting theoretical models and by highlighting hidden relationships between quantities characterizing the observed phenomena. The present article is therefore devoted to the analysis of synchronization experiments in magnetically controlled plasmas at JET, involving a 'target' quantity (sawteeth) and a 'driver' (modulated injected radio frequency) one. The typical approach to such analysis would start from assuming that the coupling between driver and target is free from external influences. However, since sawteeth can occur naturally and constitute a confounding factor in the analysis, by relaxing such an assumption a more realistic description of the system can emerge. The use of the conditional joint recurrence plots, complemented by the conditional transfer entropy, has provided further evidences supporting the effective influence of the pacing on the fast ions populations of both the minority and of the main plasma species in H-mode plasmas. The results highlight specific physical factors affecting the efficiency of the pacing and are in agreement with modelling estimates. The analysis performed then paves the way for future studies on more recent DT pulses performed at JET, and on data from other synchronization experiments.

[8] See the author list of 'Overview of JET results for optimising ITER operation' by J Mailloux *et al* to be published in Nuclear Fusion Special issue: Overview and Summary Papers from the *28th Fusion Energy Conf. (Nice, France, 10–15 May 2021)*.
[*] Author to whom any correspondence should be addressed.

Keywords: sawteeth pacing, recurrence plots, conditional transfer entropy, non linear dynamics

(Some figures may appear in colour only in the online journal)

1. Introduction

Nowadays magnetically controlled nuclear fusion reactors represent the most promising configuration to produce energy for general use in the not too far future. The next generation device, ITER, is expected to operate in an operation regime commonly called H-mode [1], where the confinement time, i.e., the average time during which the plasma loses its energy, is almost twice the one of the L-mode regime. However, the plasma core of these discharges is affected by reconnection events when the safety factor decreases below one. These instabilities leave a clear signature in the main plasma parameters, particularly in the temperature, as quite evident oscillations. It has been demonstrated that too long natural sawteeth periods can result in excessively large crashes, which can constitute the seed of neoclassical tearing modes (NTM) [2]. The growth and saturation of NTMs are then well known to have the potential to lead to catastrophic events known as disruptions [3]. The simple suppression of the sawteeth, on the other hand, is probably not the best strategy in the perspective of the reactor, because they can contrast the accumulation of both ashes and impurities, which could lead to the consequent poisoning of the plasma core.

Recently, it has been observed at JET how notches in the ion cyclotron resonance heating (ICRH) scheme can effectively be used to pace sawteeth in L-mode discharges, by influencing the fast ions distribution of the minorities injected; the results have been quantified with both advanced and simple statistical techniques [4].

The H-mode phase is in general more complicated to analyse. However, very good results have been described in [5] implementing advanced statistical tools, such as the transfer entropy (TE) and the convergent cross mapping [6]. In particular, the amount of Shannon information shared between the quantity denoted as the driver, the ICRH, and the response one, the electron temperature in the core (Te), was quantified. The main limitation of such estimators lies in the underlying hypothesis that only the considered driver, i.e., the ICRH, is influencing the observable response, i.e. the central electron temperature. In this paper then, an original statistical tool, the conditional joint recurrence plots (CJRP) [7], has been applied to DD pulses during H-mode phases, to describe the ICRH pacing, by taking into consideration also the possible occurrence of natural sawteeth. This analysis is complemented by a more traditional technique, used already in the past to address this type of situations: the so-called conditional transfer entropy (CTE) [8].

This article is structured as follows. Section 2 provides a brief description of the pacing technique, and then section 3 describes the CJRP and the CTE, while section 4 shows the analysis performed as well as the estimates provided by the modelling code considered, i.e., the PION code [9], before drawing the conclusions.

2. Overview of sawteeth pacing experiments

Sawteeth are the visible effects on the main plasma parameters of the periodical relaxation of internal kink modes [10]. As stated previously, it has been observed experimentally [2] that too long sawteeth periods can lead to large crashes with deleterious effects on the plasma confinement and even to its stability. Consequently, to keep their beneficial effects, related to the expulsion of He ashes and impurities, as shown in [11] and in agreement with simulations [12], sawteeth pacing experiments have been performed and have demonstrated in the last years their effectiveness [4, 11]. The objective of such experiments consists of triggering sawteeth crashes at specific rates in order to preserve their positive effects and reduce or avoid the unwanted consequences [4].

According to [13, 14] the basic condition for a sawtooth to occur, can be summarized in terms of the shear $\left(s = \frac{r}{q}\frac{\mathrm{d}q}{\mathrm{d}r}\right)$ at the $q = m = n = 1$ surface, where m and n are the poloidal and toroidal mode numbers, as follows:

$$s|_{q=1} > \max\left(s_{\mathrm{crit}}, \delta\widehat{W}\right) \tag{1}$$

where s_{crit} is a critical shear value depending on physical quantities in a narrow layer close to the $q = 1$ surface [13], while $\delta\widehat{W}$ stands for the normalized potential energy:

$$\delta\widehat{W} \propto \frac{\delta W}{s_1 \xi^2} \tag{2}$$

where ξ represents the radial displacement inducing the perturbation, i.e. $\xi \simeq e^{im\left(\theta - \frac{n}{m}\phi\right)}$. Specifically then:

$$\delta W = \delta W_{\mathrm{core}} + \delta W_{\mathrm{fast}} \tag{3}$$

Considering equations (2) and (3), to implement the pacing, two typologies of experiments had been historically conducted and have been aimed at either altering the shear close to the $q = 1$ surface $\left(s_1 = s\,|_{q=1}\right)$ [15], or at modifying the fast ion population and consequently the δW_{fast} term [4, 11]. The former type is based on modifying the local plasma parameter and the current profile close to the $q = 1$ surface with the use of an external heating, such as the electron cyclotron heating [15]. The latter instead, is based on the injection of a minority species in the plasma and on a ICRH heating scheme [4, 11]. Results had been obtained by both varying the ICRH antenna phasings [11], or by directly notching the ICRH [4].

To consolidate the conclusions, which can be derived from these experiments, a statistical evaluation of the correlation between the fast ion populations and the ICRH is therefore of great interest.

3. CTE and CJRP

In this section, the two main statistical estimators, the CJRP and the CTE, are described in sections 3.1 and 3.2 respectively.

3.1. Recurrence plots and conditional recurrence plots

A recurrence plot (RP) is a binary plot of a matrix, having ones when the phase space trajectory of an attractor visits at different time instances the same area in its phase space within a certain threshold [16]. Mathematically this can be expressed by the Heaviside function in equation (4) where the definition of the recurrence matrix RP_y, for the generic time series 'y', has been made explicit. Each element of such matrix then can be estimated as:

$$\mathrm{RP}_y = \mathrm{RP}^{y}_{ij} = \Theta\left(\varepsilon - \|\boldsymbol{y}_i - \boldsymbol{y}_j\|\right), \boldsymbol{y}_{i,j} \in R^m,\ i,j \in 0,N \quad (4)$$

where N stands for the number of elements in the time series 'y', 'm' for the dimension of the embedded phase space, ε is a threshold limit, optimally set according to [7], and finally $||u||$ represents a chosen norm. Three illustrative examples of RPs are reported in figure 1: a white noise time series (figure 1(A)), a Lorentz system (figure 1(B)) [17] and a logistic map (figure 1(C)) [18].

By taking the Hadamard product $(\odot)$ of the matrices describing two or 'n' RPs, the simultaneous occurrences between different quantities or dynamical systems are preserved in the most widely used extension of the RPs: the joint recurrence plots (JRP) [7]

$$\mathrm{JRP}_{xyz} = \overbrace{\mathrm{RP}_x \odot \mathrm{RP}_y}^{\mathrm{JRP}_{xy}} \odot \mathrm{RP}_z \quad (5)$$

Recently, the so-called conditional recurrence plots [19] has also been proposed

$$\mathrm{CJRP}_{xy|z} = \mathrm{JRP}_{xy} \odot (1 - \mathrm{JRP}_{zy}) \quad (6)$$

As stated above, equation (5) can be used to estimate simultaneous occurrences among three quantities, but it cannot distinguishes the relative influence among the three. Equation (6) instead has been meant to sift out the confounding influence of 'z' on 'y' in order to highlight more clearly the one between 'x' and 'y'. Technical details can be found in [19], but the main idea behind the CJRP in equation (6) is that of reducing progressively $\varepsilon_{\mathrm{JRP}_{zy}}$ while keeping the optimal value for $\varepsilon_{\mathrm{JRP}_{xy}}$. Indeed, to recurrences in JRP_{zy}, due to points that are close on the attractors of 'z' and 'y', a value of '1' is assigned in the matrix of the JRP_{zy}, but are then discarded in the $\mathrm{CJRP}_{xy|z}$ matrix, in which they assume a value of '0', because of the mathematical definition of the CJRP themselves. The outcome then highlights the occurrences between 'x' and 'y' while the ones between 'z' and 'y' are filtered out step by step by the iterative reduction of the threshold $\varepsilon_{JRP_{zy}}$. The confounding influence of 'z' on 'y' for the inference analysis is therefore minimized.

Finally, by varying the delay between 'x' and 'y', it is possible to estimate the lag-time, which corresponds to the highest degree of synchronization between the two times series.

Figure 1. Three illustrative RPs: (A) white noise; (B) Lorentz system [17]; (C) logistic map [18].

Indeed, starting from the topological properties of RPs and their extensions, a set of estimators have been defined by the recurrence quantification analysis [20]. In the following, the so-called *Determinism* (DET) has been used to capture the pieces of information regarding the coupling between dynamic processes [7]. DET is based on the distribution of diagonals, which are the visible representations of trajectories of the attractor passing through the same region of the phase space, but at different times. Consequently, short ones stand for weak correlations, chaotic or stochastic processes, while long diagonals are typical of deterministic systems. DET in equation (7) is then defined as the percentage of recurrence points forming the diagonal lines [7, 20]:

$$\mathrm{DET} = \frac{\sum_{l=l_{\min}}^{N} lP(l)}{\sum_{l=1}^{N} lP(l)} \quad (7)$$

In equation (7), 'N' stands for the number of elements in the time series, 'l' for the length of a specific diagonal line and $P(l)$ for the number of diagonals with the considered length 'l'. $l_{\min}$ is customary set to '2' [7, 16]. In this work the already validated CRP tool [16] has been used to compute the RP, the CJRP and the considered estimator described above, the DET.

3.2. TE and CTE

The CTE [8] is a natural extension of the TE [21], which is one of the most widespread tool to estimate the information flow, from a candidate 'driver' or 'source', 'x', to a 'receiver' or 'target', 'y', in terms of information transfer [22]. The TE quantifies the amount of information about 'y' that can be gained by knowing 'x'. This information can help predicting the future of the targeted 'y' beyond what could be possibly be done using only its past. Such eventual improvement is therefore equated to the effective influence of 'x' on 'y'.

In case of time series, the TE is calculated modelling the signals as discrete Markov processes of order 'k' and 'l'. This means that the probability of measuring a specific value for each quantity considered at the time instance '$n+1$' depends in principle only on 'k' and 'l' previously observed states of the quantities themselves [8]. Therefore, the TE can estimate the relative importance of a quantity $\boldsymbol{x}^{(k)}$ to estimate the state y_{n+1} of another process $\boldsymbol{y}^{(l)}$, while considering also the memory of y itself. Mathematically the TE represents the conditional mutual information $I(u|v)$ in equations (8) and (9) between $\boldsymbol{x}^{(k)}$ and $\boldsymbol{y}^{(l)}$. The CTE then, simply includes a further quantity

$z^{(m)}$ as a possible influence of the outcome of the receiver or 'response' quantity $y^{(l)}$ [8]:

$$\mathrm{TE}_{X\to Y} = I\left(x_n^{(k)}, y_{n+1}|y_n^{(l)}\right) \tag{8}$$

$$\mathrm{CTE}_{X\to Y|Z} = I\left(x_n^{(k)}; y_{n+1}|y_n^{(l)}, z_n^{(m)}\right) \tag{9}$$

Equation (8) can be written for discrete quantities as [21]:

$$\mathrm{TE}_{X\to Y} = \sum p\left(y_{n+1}, x_n^{(k)}, y_n^{(l)}\right)\log_2\left(\frac{p\left(y_{n+1}|x_n^{(k)}, y_n^{(l)}\right)}{p\left(y_{n+1}|y_n^{(l)}\right)}\right) \tag{10}$$

In equation (10) it is clear than that if $x_n^{(k)}$ does not improve the understanding of y_{n+1}, i.e. $p\left(y_{n+1}|x_n^{(k)}, y_n^{(l)}\right) = p\left(y_{n+1}|y_n^{(l)}\right)$, then TE = 0. Using the same formalism of equation (10), an expression for the CTE has been provided in equation (11); further, details can be found in [23, 24] about the formal definition of the CTE.

$$\mathrm{CTE}_{X\to Y|Z} = \sum p\left(y_{n+1}, x_n^{(k)}, y_n^{(l)}, z_n^{(m)}\right) \cdot \log_2\left(\frac{p\left(y_{n+1}|x_n^{(k)}, y_n^{(l)}, z_n^{(m)}\right)}{p\left(y_{n+1}|y_n^{(l)}, z_n^{(m)}\right)}\right) \tag{11}$$

The influence of the selected quantities $x_n^{(k)}$ and $z_n^{(m)}$ on $y_n^{(l)}$ can be studied also at a differently spaced time instances of delays d_{xy} or d_{zy}. Both the TE and the CTE are consequently estimators to be maximized.

For continuous quantities, the definitions of the TE and CTE are conceptually the same and their description would not improve the understanding of the estimators themselves or of their underlying ideas. However, it is worth considering that the main issue in the estimation of the entropies in equations (10) and (11) are the estimates of the probability density functions *pdfs*. The Kraskov, Stögbauer and Grassberger estimator is one of the most widespread methodology to tackle such issue, thanks to the use of the digamma function. Details can be found in [25, 26].

In this work, the consolidated JIDT tool [27] has been used for both the TE and the CTE.

4. Analysis of H-mode discharges

In this section, the main results obtained with the previously described estimators are reported. It is important to stress that the values of the delays, at which maxima of the considered estimators are observed, are to be considered as the time windows during which the ICRH itself exerts most of its influence on the time evolution of the sawteeth. In other words, the ICRH notching is expected to influence the fast ion population mainly within the time windows ending with this maximum value of the indicators [28–30]. This time interval corresponds to the slowing down time of the ions [4, 5], i.e. the time interval taken by the ions to thermalize on the electrons of the plasma, both for the minority and for the main plasma species.

Table 1. Main parameters for the pulses (P) considered in this analysis, including the reference (R) ones. All pulses have been conducted at $I = 2.2$ MA and Bt = 2.8 T. The pulse 94087 differs from the 94088,89 ones (underlined in the table below together with the corresponding reference pulse) by the different percentage of minorities (H%).

Pulse P/R	n_e (10^{19} m^{-2})	P_{NBI} (MW)	P_{ICRH} (MW)	v_{ICRH} (MW)	H (%)
94087 P	11.8	20.5	5.7	3	2.7
94091 R	10.9	20.0	5.8		2.7
94088 P	11.1	20.3	6.2	3	1.3
94089 P	11.4	20.0	6.1	2.5	1.2
94090 R	11.0	20.0	5.3		1.7

Section 4.1 provides a short overview of the pulses considered and of the expected estimates obtained using the PION code for the evaluation of the slowing down time of the fast ions, while section 4.2 provides the results obtained using the CTE and the CJRP in relation to the PION estimates.

4.1. Experimental discharges considered in the analysis and expected model estimates

In this article, three JET pulses, dedicated to the preparation of the ICRH scenario in support of the DT campaign, have been analysed during the stationary H-mode phases. Table 1 provides the main characteristics of the considered pulses and of the corresponding reference pulses. The main idea behind the use of reference pulses is simple. Since sawteeth are quasi-periodic and can occur naturall. Also during pacing experiments, we have tried to decouple the naturally occurring crashes from the paced ones by using the measurements of the reference pulses. In more detail, for the driver *'x'*, we have considered the total ICRH power injected, while the response quantity *'y'*, describing both paced and natural sawteeth, is the central electron temperature measured by the ECE diagnostic. Finally, the Te measured for the reference pulse, *'z'*, has been used to describe the occurrence of natural sawteeth. Figure 2 shows an example comparing the time traces of the pulse 94089 with the 94090 used as reference.

Experimentally an excellent pacing of the sawteeth for the 94089 pulse was achieved, while the pacing efficiency was not optimal for shot number 94087 and poor for shot number 94088.

One of the possible explanations for such different behaviours is the actual influence of the main plasma second harmonic that absorbs part of the injected power [4]. In other words, not only the minorities, but also the fast ion population of the main ion species might influence the experimental output.

To interpret the main results obtained with the estimators used, the PION code has been run to determine the main quantities related to the fast ion populations, especially the slowing down time of the fast ions on the electrons.

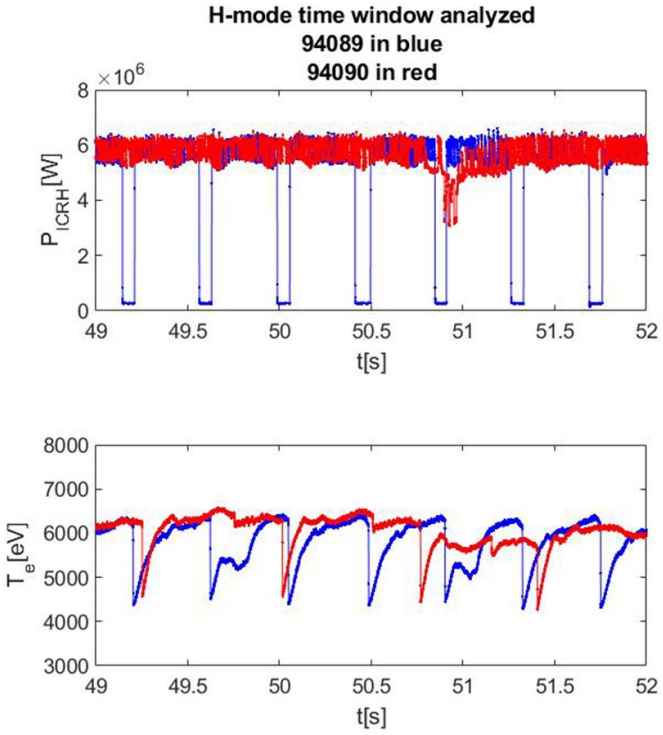

Figure 2. TOP: Total injected ICRH power for the pulse 94089 in blue and for the reference pulse 94090 in red; bottom: central electron temperatures, where natural sawteeth can be observed in red for the 94090 time trace and paced ones for the 94089 in blue.

Table 2. Main estimates for the slowing down time of ions on electrons for the two main species of the plasma, the hydrogen minority and deuterium at the resonance position.

Pulse	$\tau_{eH} \pm \sigma_{\tau_{eH}}$ (ms)	$\tau_{eD} \pm \sigma_{\tau_{eD}}$ (ms)
94087	(266 ± 40)	(531 ± 80)
94088	(260 ± 25)	(519 ± 50)
94089	(234 ± 26)	(468 ± 52)

For these three pulses, the first harmonic of the hydrogen ions ('H1' from now), the second one of deuterium ions ('D2' from now on) and the electrons adds up to 99.9% of the damping power of the ICRH. Furthermore, during the time window considered for the analysis, both resonances overlap at $R \sim 3$ m, i.e. $\psi \sim 0; 0.05$ where ψ stands for the normalized flux function. Table 2 provides the PION estimates of the slowing down time of hydrogen and deuterium on the electrons.

4.2. Results obtained using the selected estimators CTE and CJRP

In this subsection, the results obtained by the application of the CTE and of the CJRP are shown. The analysis has been performed over one period of the ICRH frequency, i.e. the delay between the ICRH and the Te time trace has been varied from $[0, 1/\nu_{ICRH}]$, to avoid duplicating the results over a wider time window.

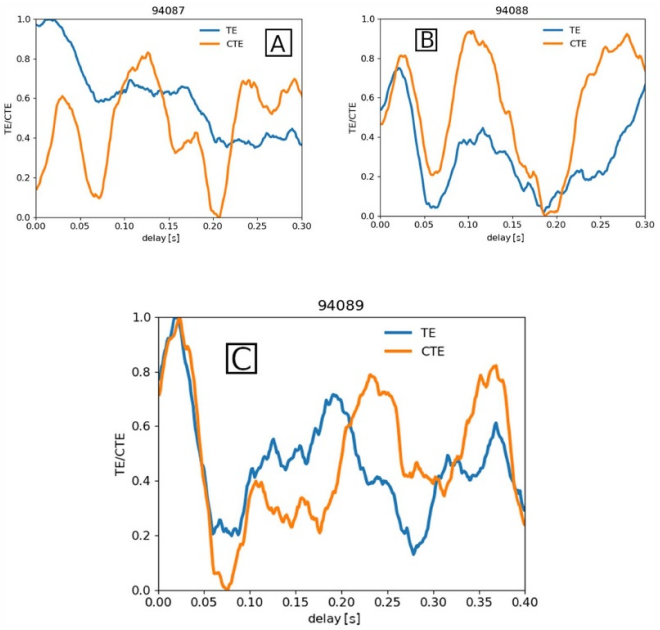

Figure 3. CTE and TE results for the three pulses considered. (A) 94087: two peaks at 127 ms and 240 ms can more clearly be observed using the CTE w.r.t. the TE, which shows only the ∼20 ms peak; (B) 94088: the peaks at 110 ms and at 255 ms are intensified by the use of the CTE w.r.t. the TE where only the ∼20 ms peak emerges also in this pulse; (C) 94089: using the CTE the two peaks at 236 ms and 380 ms are easier to be identified w.r.t. the TE which shows again only the ∼20 ms one.

The CTE results are reported in figure 3 where also the TE is shown for comparison. As seen by simple inspection of these plots, the CTE improves the clarity of the results w.r.t. the TE, but no definitive conclusion can be drawn. It is interesting to note that all pulses reveal clearly the importance of the ICRH on the pacing sawteeth for time windows compatible with the slowing down time of the hydrogen (see table 2). However, also a strong influence in other time windows, which cannot be directly linked to the fast ions properties, emerges.

A clearer and more comprehensive explanation of the experimental observations can be derived with the CJRP, considering the behaviour of the DET shown in figure 4.

Pulse 94089 clearly shows two main peaks related to the ICRH. The first one corresponds to the slowing down time of the hydrogen ions, due to the absorption at the H1 harmonic, while another peak can be observed within the lower bound of the estimate of the slowing down time of the deuterons, due to the D2 harmonic absorption.

On the other hand, even if both pulses 94088 and 94087 show the importance of the H1 harmonic, also other local peaks, not easily related to the fast ion populations, can be observed.

Consequently, the results in figure 4 provide a quite coherent description and allow drawing a series of conclusions, as reported in the following section.

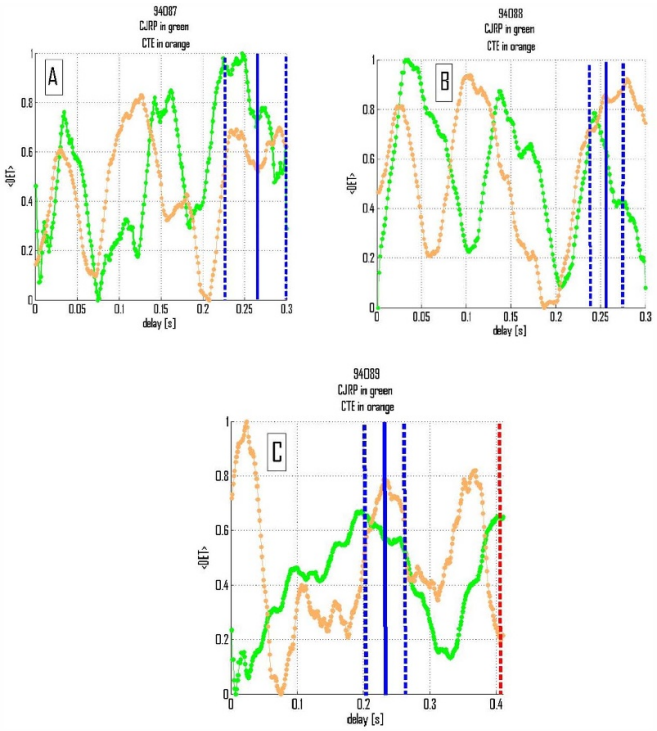

Figure 4. Normalized DET results for the three pulses considered superimposed on normalized CTE results. In blue the estimates and in dashed blue the corresponding upper and lower bounds for H1; in red and dashed red the D2 ones. (A) 94087: the H1 peak has higher relevance w.r.t. the previous ones detected; (B) 94088: the H1 peak has lower relevance w.r.t. previous ones detected; (C) 94089 shows the importance of the D2 and of the H1.

5. Conclusions

In this article, two estimators have been used to support the analysis of dedicated experiments of sawteeth pacing with ICRH modulation: the new CJRP and the more traditional CTE. Both have been implemented to infer the influence of a driving observable (ICRH) on a target (Te with paced and natural sawteeth) minimizing the influence of a third quantity (reference Te with natural sawteeth).

Of the two, the CJRP provides a more coherent description of the analysis performed. Due to the non-trivial optimization of the estimator, the results of the CTE have been used only to support the CJRP conclusions.

The results shown in figure 4 illustrate clearly how pulse 94089 has been properly optimized for the pacing both in term of minority and ICRH modulation. The reported evidence also supports the idea that the ICRH has been able to influence both the minority (H) and the main fast ion distributions (D) of the plasma by the first and the second harmonics respectively.

The results for pulses 94087 and 94088, while not being as clear as the 94089 ones, providing, in any case some interesting preliminary information to be considered in comparison with the 94089. Keeping in mind the fact that pulse 94088 differs from the 94089 in the ICRH frequency and from the discharges 94087 and 94089 in both the frequency and the minority concentration used, then the study performed leads to two alternatives: (a) a not optimized ICRH, in terms of either ICRH frequency or minority concentration in the plasma, can lead to effects on the fast ion populations theoretically not yet considered and that cause the poor pacing observed for the 94088 and the not optimal pacing of the 94087 (the difference due to the different minority concentration); (b) other physical quantities influence the sawteeth occurrences of the paced pulses, i.e. not all spurious influences on the central electron temperature of the paced pulses have been considered.

While the former case goes far beyond the scope of this article, further studies will be dedicated to share some light on the latter hypothesis thanks to the CJRP potential to easily include further quantities in the analysis.

In any case, the different behaviours of the CJRP results in figure 4 between pulse 94088 and pulse 94087 can partially explain the poor pacing of discharge 94088 observed experimentally. Considering figure 4(B) in fact the relative importance of the third peak related to the hydrogen fast ion population is lower w.r.t. the two others detected, the opposite occurring for the 94087 discharge.

The results obtained are in any case very promising and, therefore, they are expected to provide useful hints for the analysis of the DT2 campaign of JET on specific experiments with ICRH modulations.

Data availability statement

The data that support the findings of this study are available upon reasonable request from the authors.

Acknowledgments

This work has been carried out within the framework of the EUROfusion Consortium, funded by the European Union via the Euratom Research and Training Programme (Grant Agreement No. 101052200—EUROfusion). Views and opinions expressed are however those of the author(s) only and do not necessarily reflect those of the European Union or the European Commission. Neither the European Union nor the European Commission can be held responsible for them.

ORCID iDs

Emmanuele Peluso https://orcid.org/0000-0002-6829-2180
Teddy Craciunescu https://orcid.org/0000-0002-0012-4260
Michela Gelfusa https://orcid.org/0000-0001-5158-7292
Daniel Gallart https://orcid.org/0000-0003-1663-3550
David Taylor https://orcid.org/0000-0002-0465-2466

References

[1] Wagner F *et al* 1982 *Phys. Rev. Lett.* **49** 1408–12
[2] Chapman I T *et al* 2010 *Nucl. Fusion* **50** 102001
[3] De Vries P *et al* 2011 *Nucl. Fusion* **51** 053018
[4] Lerche E *et al* 2017 *Nucl. Fusion* **57** 036027

[5] Murari A *et al* 2017 *Nucl. Fusion* **57** 126057
[6] Sugihara G *et al* 2012 *Science* **338** 496–500
[7] Marwan N *et al* 2007 *Phys. Rep.* **438** 237–439
[8] Bossomaier T *et al* 2016 *An Introduction to Transfer Entropy* (Berlin: Springer) (https://doi.org/10.1007/978-3-319-43222-9)
[9] Eiksson L G *et al* 1993 *Nucl. Fusion* **33** 1037
[10] Igochine V 2015 *Active Control of Magneto-Hydrodynamic Instabilities in Hot Plasmas* (Berlin: Springer) (https://doi.org/10.1007/978-3-662-44222-7)
[11] Graves J P *et al* 2015 *Plasma Phys. Control. Fusion* **57** 014033
[12] Nicolas T *et al* 2014 *Phys. Plasmas* **21** 012507
[13] Porcelli F, Boucher D and Rosenbluth M N 1996 *Plasma Phys. Control. Fusion* **38** 2163
[14] Chapman I T, Igochine V, Maraschek M, McCarthy P J and Tardini G 2013 *Plasma Phys. Control. Fusion* **55** 065009
[15] Angioni C, Goodman T P, Henderson M A and Sauter O 2003 *Nucl. Fusion* **43** 455
[16] Marwan N and Kurths J 2002 *J. Phys. Lett.* A **302** 299–307
[17] Krakovská A *et al* 2016 (available at: https://arxiv.org/pdf/1511.00505.pdf)
[18] May R 1976 *Nature* **261** 459
[19] Peluso E, Craciunescu T and Murari A 2020 *Entropy* **22** 865
[20] Zblut J P *et al* 2006 *Wiley Encyclopedia of Biomedical Engineering* ed M Akay (Hoboken, NJ: Wiley) (https://doi.org/10.1002/9780471740360.ebs1355)
[21] Schreiber T 2000 *Phys. Rev. Lett.* **85** 461–4
[22] Jakubowski M H, Steiglitz K and Squier R 1997 *Phys. Rev.* E **56** 7267
[23] Lizier J T, Prokopenko M and Zomaya A Y 2010 *Chaos* **20** 037109
[24] Lizier J T *et al* 2008 *Phys. Rev.* E **77** 026110
[25] Kraskov A, Stögbauer H and Grassberger P 2004 *Phys. Rev.* E **69** 066138
[26] Kozachenko L *et al* 1987 *Probl. Inf. Transm.* **23** 9–16
[27] Lizier J T 2014 *Front. Robot.* AI **1** 11
[28] Murari A, Peluso E, Gelfusa M, Garzotti L, Frigione D, Lungaroni M, Pisano F and Gaudio P 2016 *Nucl. Fusion* **56** 026006
[29] Murari A, Craciunescu T, Peluso E, Gelfusa M, Lungaroni M, Garzotti L, Frigione D and Gaudio P 2016 *Nucl. Fusion* **56** 076008
[30] Murari A, Lungaroni M, Peluso E, Gaudio P, Lerche E, Garzotti L and Gelfusa M 2018 *Entropy* **20** 627